Wind and Structures, *Vol. 18, No. 5 (2014) 549-566*
DOI: http://dx.doi.org/10.12989/was.2014.18.5.549

A hybrid numerical simulation method for typhoon wind field over complex terrain

Wenfeng Huang* and Huanlin Zhou

School of Civil Engineering, Hefei University of Technology, Anhui, 230009, China

(Received May 20, 2013, Revised December 20, 2013, Accepted February 14, 2014)

Abstract. In spite of progress in the numerical simulation of typhoon wind field in atmospheric boundary layer (ABL), using typhoon wind field model in conjunction with Monte Carlo simulation method can only accurately evaluate typhoon wind field over a general terrain. This method is not enough for a reliable evaluation of typhoon wind field over the actual complex terrain with surface roughness and topography variations. To predict typhoon wind field over the actual complex terrain in ABL, a hybrid numerical simulation method combined typhoon simulation used the typhoon wind field model proposed by Meng *et al*. (1995) and CFD simulation in which the Reynolds averaged Navier-Stokes (RANS) equations and *k*-*ε* turbulence model are used. Typhoon wind filed during typhoon Dujuan and Imbudo are simulated using the hybrid numerical simulation method, and compared with the results predicted by the typhoon wind field model and the wind field measurement data collected by Fugro Geotechnical Services (FGS) in Hong Kong at the bridge site from the field monitoring system of wind turbulence parameters (FMS-WTP) to validate the feasibility and accuracy of the hybrid numerical simulation method. The comparison demonstrates that the hybrid numerical simulation method gives more accurate prediction to typhoon wind speed and direction, because the effect of topography is taken into account in the hybrid numerical simulation method.

Keywords: typhoon wind field; complex terrain; CFD simulation; field measurement data; comparison

1. Introduction

Up until to now, using typhoon wind field model in conjunction with Monte Carlo simulation method has been commonly used in the typhoon wind field simulation in atmospheric boundary layer (ABL). This method was first suggested by Russell (1971) and developed by Tryggvason *et al*. (1976), Batts *et al*. (1980), Georgiou (1985), Vickery and Twisdale (1995), Vickery *et al*. (2009). In spite of progress in the numerical simulation of typhoon wind field in ABL, using typhoon wind field model in conjunction with Monte Carlo simulation method can only accurately evaluate typhoon wind field over a general terrain. But it is not enough for a reliable evaluation of typhoon wind speed over the actual complex terrain with surface roughness and topography variations.

Conventionally, for the actual complex terrain, the practitioner will be recommended to do a physical simulation in a boundary layer wind tunnel. Topographic studies in wind tunnels could be performed to ascertain wind field at the site surrounded by complex terrain but upstream wind

*Corresponding author, Ph. D., E-mail: wfhuang@163.com

http://www.techno-press.org/?journal=was&subpage=8 ISSN: 1226-6116 (Print), 1598-6225 (Online)

field should be simulated first. The upstream wind field is often simulated according to that specified in wind standards and codes, which is only an approximation to the real typhoon wind field (Chock and Cochran 2005). On the other hand, the computational fluid dynamics (CFD) are also applied to evaluate wind fields over simple or complex terrain for given upstream wind fields, such as Bitsuamlak *et al*. (2004), Tamura *et al*. (2007), Lee *et al*. (2010), Wakes *et al*. (2010). The motivation of a study is thus raised from such a question: can we integrate typhoon wind field model and CFD simulation to provide a better prediction of typhoon wind field for a site surrounded by complex terrain?

In this regard, this paper thus develops a hybrid numerical simulation method to evaluate the typhoon wind field over actual complex terrain considering topography influence and surface roughness length. This paper is organized as follows: First, the hybrid numerical simulation method is introduced, including: 1) typhoon wind field model; 2) upstream typhoon wind fields of complex terrain generated by the typhoon wind field model together and typhoon key parameters; 3) typhoon wind fields at the site obtained by using the CFD simulation and upstream typhoon wind fields setting as inputs. Then, the complex terrain around the Stonecutters Bridge in Hong Kong is chosen for the study whose topographic feature is very complex. Typhoon wind filed during typhoon Dujuan and Imbudo are simulated using the hybrid numerical simulation method, and compared with the results predicted by the typhoon wind field model and the wind field measurement data collected by Fugro Geotechnical Services (FGS) in Hong Kong at the bridge site from the field monitoring system of wind turbulence parameters (FMS-WTP) to validate the feasibility and accuracy of the hybrid numerical simulation method.

2. Hybrid numerical simulation method

2.1 Typhoon wind field model

The typhoon wind field model proposed by Meng *et al*. (1995) is used in this study. The basic equations of the typhoon wind field model are given as follows

$$\frac{d\boldsymbol{v}}{dt} = -\frac{1}{\rho}\nabla p - f\boldsymbol{k}\times\boldsymbol{v} + \boldsymbol{F} \tag{1}$$

$$p = p_0 + \Delta p_0 \exp[-(r_m / r)^B] \tag{2}$$

where $\boldsymbol{v}$ is the wind velocity; $\boldsymbol{k}$ is the unit vector; $\boldsymbol{F}$ is the friction force; ∇ is the two-dimensional del operator; p is the atmospheric pressure; ρ is the air density; f is the Coriol is parameter; p_0 is the central pressure;Δp_0 is the central pressure difference equal to p_m-p_0;p_m is the ambient pressure (theoretically at infinite radius); $r_{\max}$ is the radius to maximum wind; r is the radial distance from the typhoon center; and B is the Holland's radial pressure profile parameter, taking on values between 0.5 and 2.5.

If the typhoon makes landfall, a typhoon decay model shall be included in the basic equations of the typhoon wind field model (Vickery and Twisdale 1995). The basic equations of the typhoon wind field model can be solved by using the wind decomposition method (Meng *et al*. 1995).

2.2 Upstream typhoon wind fields of complex terrain

To simulate upstream typhoon wind fields with consideration of the interaction between typhoon winds and terrain surface roughness, the average and directional surface roughness length z_0 over the complex terrain are determined by using the Digital Elevation Model (DEM) information provided by the CGIAR (Consultative Group on International Agricultural Research) consortium together with land use information. A set of typhoon key parameters obtained from the Observatory and the computed average surface roughness length$z_0$are used as inputs to the typhoon wind field model to generate a typhoon wind field. For the typhoon wind field generated, the wind speed and direction can be identified for the field measurement site. If the directional surface roughness length identified is not the same as the average surface roughness length z_0, this set of key typhoon parameters and the directional surface roughness length shall be used to re-generate a typhoon wind field until the typhoon wind direction is consistent with the directional surface roughness length used. The wind speed and wind direction obtained by this way are regarded as the upstream typhoon wind field for the site over the complex terrain at its initial place. Then, let this typhoon move at a one-hour time interval and repeat the above procedure to obtain another upstream typhoon wind field for the site until this typhoon disappears. Therefore, a complete assembly of upstream typhoon wind fields for the site over the complex terrain can be obtained during this typhoon happens.

2.3 Typhoon wind fields at the site

The CFD simulation is used to obtaining typhoon wind fields at the site with consideration of topographic influence. In this regard, the topography of the complex terrain at the site shall be modeled with appropriate computational domain, meshes and boundary conditions. By taking upstream typhoon wind fields as an inlet to the topographic model, the CFD simulation with the Reynolds-averaged Navier-Stokes (RANS) method is performed. The typhoon wind fields at the site surrounded by the complex terrain can be obtained.

The governing equations of RANS method used in the CFD simulation for steady, incompressible flow are written as follows (Cheng *et al*. 2003)

$$\frac{\partial U_i}{\partial x_i} = 0 \tag{3}$$

$$\frac{\partial U_i U_j}{\partial x_j} = -\frac{1}{\rho}\frac{\partial P}{\partial x_i} + \frac{\partial}{\partial x_j}(\upsilon \frac{\partial U_i}{\partial x_j} - \overline{u_i' u_j'}) \tag{4}$$

Where U_i and u_i' are the mean and fluctuating velocities in the x_i direction, respectively; ρ is the reference density; P is the mean pressure; υ is the viscosity coefficient. The presence of the Reynolds stress $\overline{u_i' u_j'}$ in Eq. (4) implies that the latter are not closed. Closure requires that some models be made in prescribing the Reynolds stresses in terms of the mean flow quantities. The most popular statistical turbulence closure model is the Boussinesq type of eddy viscosity approximation that assumes a linear relationship between the turbulence stresses and the mean velocity gradients

$$-\overline{u_i' u_j'} = v_t^* \left(\frac{\partial U_i}{\partial x_j} + \frac{\partial U_j}{\partial x_i}\right) - \frac{2}{3} k \delta_{ij} \tag{5}$$

where v_t^* is the kinematic eddy viscosity; $k \equiv \frac{1}{2}\overline{u_i' u_i'}$ is the turbulence kinetic energy.

In the standard k-ε model, v_t^* is determined as

$$v_t^* = C_\mu \frac{k^2}{\varepsilon} \tag{6}$$

where ε is the dissipation of turbulence kinetic energy. The standard model uses the following transport equations for k and ε

$$\frac{\partial (U_i k)}{\partial x_j} = \frac{\partial}{\partial x_j}\left[\left(\upsilon + \frac{v_t^*}{\sigma_k}\right)\frac{\partial k}{\partial x_j}\right] + v_t^* \left(\frac{\partial U_i}{\partial x_j} + \frac{\partial U_j}{\partial x_i}\right)\frac{\partial U_i}{\partial x_j} - \varepsilon \tag{7}$$

$$\frac{\partial (U_j \varepsilon)}{\partial x_j} = \frac{\partial}{\partial x_j}\left[\left(\upsilon + \frac{v_t^*}{\sigma_\varepsilon}\right)\frac{\partial \varepsilon}{\partial x_j}\right] + C_{\varepsilon 1}\frac{\varepsilon}{k}\left(\frac{\partial U_i}{\partial x_j} + \frac{\partial U_j}{\partial x_i}\right)\frac{\partial U_i}{\partial x_j} - C_{\varepsilon 2}\frac{\varepsilon^2}{k} \tag{8}$$

The equation contains five closure constants: namely C_μ, σ_k, σ_ε, $C_{\varepsilon 1}$, $C_{\varepsilon 2}$. The standard k-ε model employs values for constants that are determined by a comprehensive data fitting over a wide range of canonical turbulent flows

$$C_\mu = 0.09 \ \sigma_k = 1.00 \ \sigma_\varepsilon = 1.30 \ C_{\varepsilon 1} = 1.44 \ C_{\varepsilon 2} = 1.92 \tag{9}$$

The turbulent diffusion of k and ε in Eqs. (7) and (8) are represented using a gradient diffusion hypothesis with the Prandtl numbers σ_k and σ_ε used to connect the eddy diffusivities of k and ε to the eddy viscosity v_t^*.

The flow chart of the hybrid numerical simulation method for predicting typhoon wind field for the site over complex terrain is displayed in Fig. 1.

3. Case study

The site of the Stonecutters Bridge in Hong Kong is chosen as a case study. This is because this bridge is an important structure (the second longest cable-stayed bridge in the world) and the bridge site is surrounded by complex terrain, as indicated by Fig. 2.

3.1 Surface roughness lengths and upstream typhoon wind fields

To obtain upstream typhoon win fields for the Stonecutters Bridge, the average and directional surface roughness lengths for the complex terrain around the bridge site shall be determined. The value of the average and directional surface roughness lengths can be estimated by using the following formula, which can be represented as

$$z_0 = \frac{\sum_{i=1}^{N} z_{0i} A_i}{A} \tag{10}$$

where z_0 is the average or directional surface roughness length; z_{oi} and A_i are the surface roughness length and area occupied by the surface roughness element i; A is the total area of complex terrain that the N elements occupy.

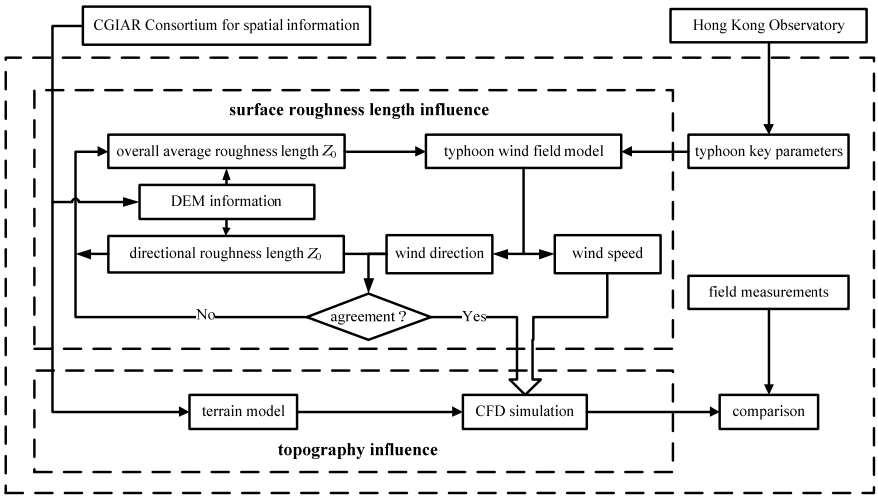

Fig. 1 Hybrid numerical simulation procedure for predicting typhoon wind field for the site over complex terrain

Fig. 2 Location of Stonecutters Bridge and its surrounding topography

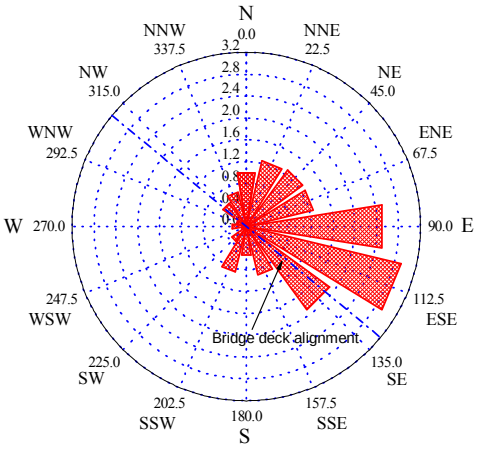

Fig. 3 Directional surface roughness length around the bridge

In this regard, the circular area taking the bridge as a center with a proper radius shall be considered (see Fig. 3). The circular area is further divided in consideration of 16 wind directions. Then, by using the DEM information and the land use information in Hong Kong, the surface roughness length z_{oi} and area A_i for each surface roughness element i with in the circular area can be determined. Accordingly, by using Eq. (10), the average and directional surface roughness length z_0 around the bridge can be estimated for different radiuses (5 km, 10 km, 20 km, 30 km) and resolutions(30 m, 60 m, 90 m). By analyzing the obtained results and in consideration of the subsequent CFD simulation, the average and directional surface roughness lengths z_0 for the area with a radius of 30 km and a resolution of 30m are used for the typhoon simulation and given in Fig. 3 and Table 1. The average surface roughness length z_0 for the entire area is 1.027 m. It can be seen that the maximum directional surface roughness length z_0 is about 2.9 m from E and ESE direction which is caused by container port terminals and Stonecutter Island in near field whereas the far field effect is induced by buildings in Kowloon and Hong Kong Island. The minimum directional surface roughness length z_0 is about 0.09 m from around WSW direction which is effected by the open sea. In summary, the directional surface roughness length z_0 can represent the spatial surface roughness element distribution for the complex terrain around Stonecutters Bridge within this circular area and can be used for obtaining upstream typhoon wind field.

Table 1 Directional surface roughness length z_0 for the complex terrain around Stonecutters Bridge

Sector	True Azimuth (degree)	z_0 (m)	Sector	True Azimuth (degree)	z_0 (m)
N	0	0.992	S	180	0.533
NNE	22.5	1.245	SSW	202.5	0.861
NE	45	1.282	SW	225	0.334
ENE	67.5	1.262	WSW	247.5	0.087
E	90	2.515	W	270	0.258
ESE	112.5	2.913	WNW	292.5	0.192
SE	135	1.882	NW	315	0.532
SSE	157.5	0.909	NNW	337.5	0.649

By using the typhoon wind field model, typhoon key parameters obtained from Observatory, the average and directional surface roughness lengths z_0, and following the procedure described in section 2.2, a complete assembly of upstream typhoon wind fields around the bridge during typhoon happens are obtained for the subsequent CFD simulation.

3.2 Topographic model and typhoon wind fields at the site

The topographic model used for CFD simulation is set up based on the DEM information provided by the CGIAR Consortium. The area of computational domain with the bridge site as a center is 38 km in East-West and 25 km in North-South. Because the highest mountain within the computational domain is 957 m high, the computational domain in the vertical direction is set as 3km so that the flow field can be fully developed. Fig. 4 shows the top view of the topographic model around the Stonecutters Bridge, and Fig. 5 displays the mesh grid for the topographic model. In horizontal level, the topographic model is meshed with 200(East-West) ×100(North-South) parts. Vertical level is divided into 80 parts, and an expansion factor 1.05 is imposed (Maurizi *et al*. 1998).A total of 1.65 million nodes are used for CFD simulation.

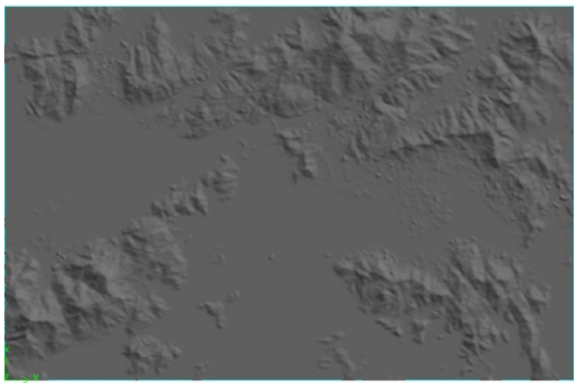

Fig. 4 Top view of topographic model

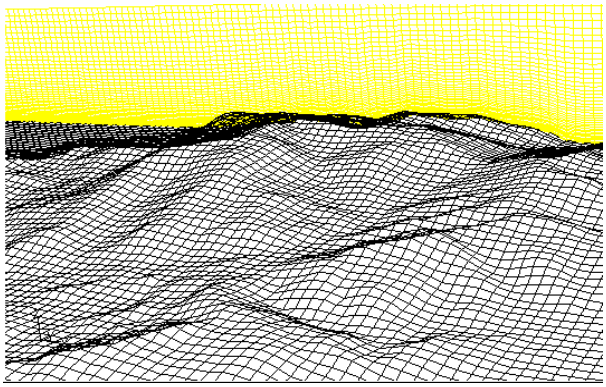

Fig. 5 Mesh grid of topographic model

Present CFD simulation has been performed with Fluent 6.3, and a general-purpose code for fluid dynamic simulations produced by Fluent Inc. The surface of the topographic model is modeled as a non-slip wall boundary. The flow inlet boundary is set as wind inlet profile with upstream wind field while the outlet boundary is specified as fully developed outflow boundary conditions. The side and top boundaries are all defined in such a way that the gradients of flow variables (including velocity and pressure) normal to those boundary faces are zero. The Reynolds-averaged Navier-Stokes (RANS) method is applied to perform CFD simulation to obtain typhoon wind fields at the bridge site, in which the finite volume method and the first order upwind scheme for spatial discretization were used and the SIMPLEC method was adopted to solve velocity and pressure simultaneously (Shen *et al.* 2003). The simulation is discontinued until residuals for all variables reach 10^{-3} accuracy and keep as constant. To make sure the correctness of the CFD simulation, an inlet profile shown in the following is used to perform a CFD simulation

$$v(z)=\begin{cases} 35\cdot(z/10)^{0.19} & z\le 500m \\ 35\cdot(500/10)^{0.13} & z>500m \end{cases} \tag{11}$$

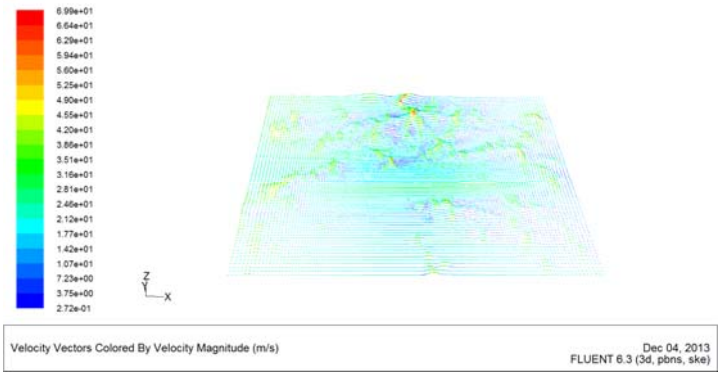

Fig. 6 Contour of velocity vectors for the surface of the topographic model during CFD simulation

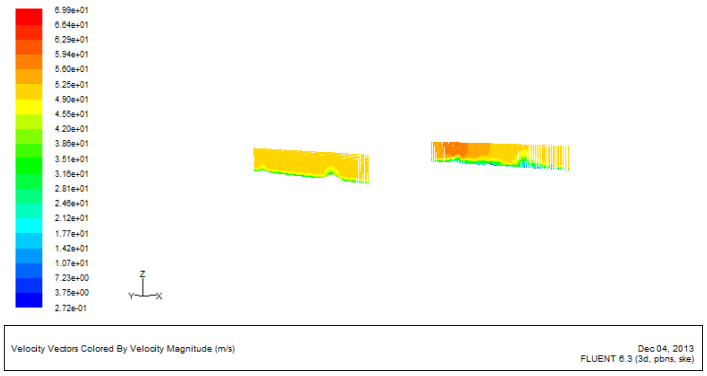

Fig. 7 Contour of velocity vectors for the front and back sides of the topographic model during CFD simulation

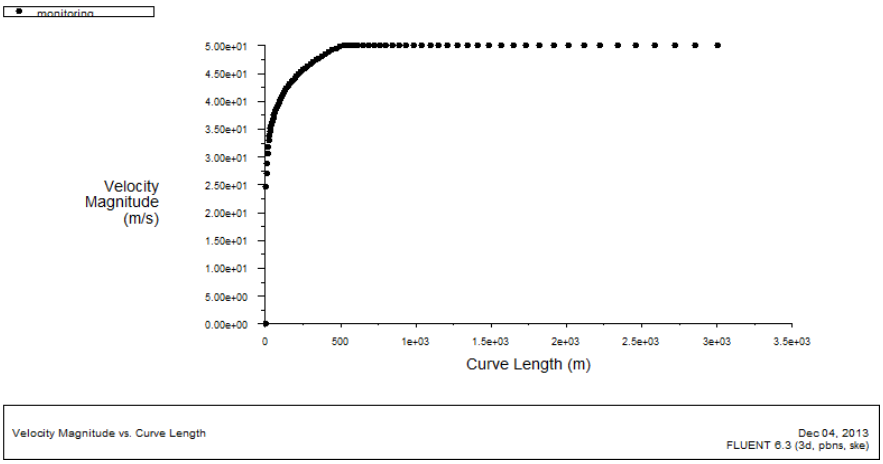

Fig. 8 Wind profile for the line near the middle part of the front for the topographic model

After the simulation, contour of velocity vectors for the surface of the topographic model is shown in Fig. 6. The contour of velocity vectors for the front and back sides of the topographic model is shown in Fig. 7. In addition, a line is created near the middle part of the front for the topographic model to observe the wind profile after CFD simulation, the wind profile for this line is shown in Fig. 8.

Therefore, by taking an upstream typhoon wind field as an inlet to the topographic model, the CFD simulation is performed. The typhoon wind field at the site surrounded by the complex terrain can be obtained. Repeating the above steps for all the upstream typhoon wind field during typhoon happens, a complete assembly of the typhoon wind fields at the site are obtained and can be used to compare with the field measurement data.

4. Comparison study

4.1 Typhoon description

4.1.1 Typhoon Dujuan

Dujuan was the first tropical cyclone that necessitated the issuance of the increasing Gale or Storm Signal No.9 since 1999 (HKO 2004). When Dujuan developed as a tropical depression over the Pacific on the early morning of 29 August, it was slow-moving. It intensified into a tropical storm on the early morning of 30 August and strengthened further into a severe tropical storm the same day. Accelerating towards the west-northwest on 31 August, Dujuan attained typhoon strength and moved towards the seas near southern Taiwan. After crossing the seas south of Taiwan on 1 September, Dujuan headed westwards towards the South China coast. The maximum sustained wind speed near its center reached 175 km/h. Dujuan entered the South China Sea on the early morning of 2 September and moved westwards towards the coast of Guangdong. While crossing the northern part of the South China Sea, it exhibited a double eye wall structure. The diameters of the inner and outer eyes were about 20km and 100km respectively. On the night of 2

September, Dujuan skirted the north of Hong Kong and hit Shenzhen. It then continued to move westwards crossing Guangdong. Dujuan weakened rapidly into a tropical storm on the morning of 3 September and became an area of low pressure over Guangxi afterward. Fig. 9 shows the track of typhoon Dujuan. Fig. 10 shows the track of typhoon Dujuan near Hong Kong.

4.1.2 Typhoon Imbudo

Imbudo developed as a tropical depression about 730 km southwest of Guam on 17 July (HKO 2004). Tracking mainly towards the west-northwest, it intensified into a tropical storm the same night. Imbudo attained severe tropical storm intensity on the morning of 19 July and further strengthened into a typhoon the next morning. The maximum sustained wind speed near its centre reached 185 km/h on 21 July. It entered the South China Sea on the night of 22 July and continued to move west-northwestwards towards the South China coast. On the morning of 24 July, it made landfall near Yangjiang of western Guangdong and weakened into a severe tropical storm that afternoon. Imbudo weakened into a tropical storm over land on the morning of 25 July and then dissipated in Guangxi the same way. Fig. 11 shows the track of typhoon Imbudo. Fig. 12 shows the track of typhoon Imbudo near Hong Kong.

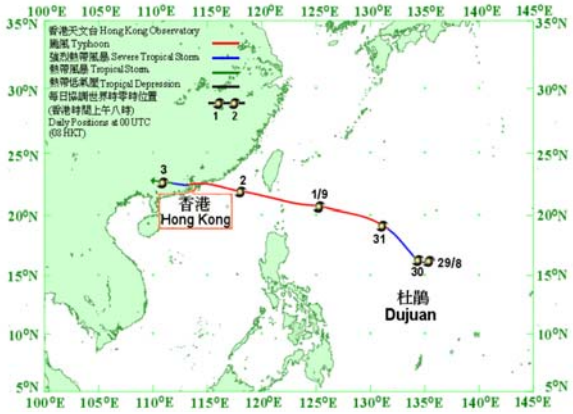

Fig. 9 Track of typhoon Dujuan: 29 August-3 September 2003

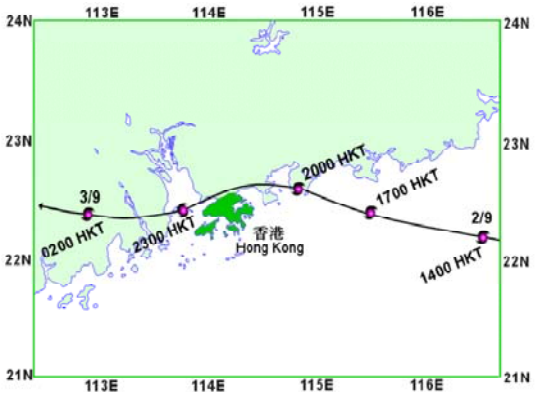

Fig. 10 Track of typhoon Dujuan

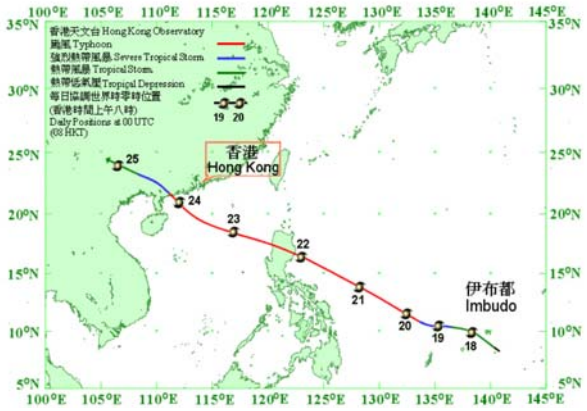

Fig. 11 Track of typhoon Imbudo: 17-25 July 2003

Fig. 12 Track of typhoon Imbudo near Hong Kong

4.1.3 Typhoon key parameters

During typhoon Dujuan and Imbudo, the typhoon warnings (signal number 3 and higher) raised by the HKO from October 2002 to September 2003 are listed in Table 2. The duration time from 00:00, 23 July 2003 to 23:00, 24 July 2003 for typhoon Imbudo and from 00:00, 1 September 2003 to 00:00, 3 September 2003 for typhoon Dujuan are selected to proceed the typhoon wind field simulation which incorporates the time range of typhoon warnings listed in Table 2 except the time range for the typhoon parameters not recorded by the HKO. The parameters of typhoon Dujuan and Imbudo are summarized in Table 3. The central pressure difference Δp_0 is calculated using a periphery pressure of 1010 hPa. The typhoon movement direction β turn clockwise from North direction. In order to simulate the typhoon wind field at an hourly interval, all the parameters are linearly interpolated from the available 6-hourly information.

Table 2 Typhoon warnings raised by HRO (Oct. 2002 to Sep. 2003)

Intensity	Name	Signal	Issuing		Cancelling		Duration hh mm
			hh mm	Dd/mon/yyyy	hh mm	Dd/mon/yyyy	
Typhoon	IMBUDO	3	13:40	23/Jul/2003	22:40	23/Jul/2003	09 00
Typhoon	IMBUDO	8NE	22:40	23/Jul/2003	05:15	24/Jul/2003	06 35
Typhoon	IMBUDO	8SE	05:15	24/Jul/2003	08:15	24/Jul/2003	03 00
Typhoon	IMBUDO	3	08:15	24/Jul/2003	12:40	24/Jul/2003	04 25
Typhoon	KROVANH	3	11:30	24/Aug/2003	11:30	25/Jul/2003	24 00
Typhoon	DUJUAN	3	10:40	02/Sep/2003	14:20	02/Sep/2003	03 40
Typhoon	DUJUAN	8NW	14:20	02/Sep/2003	20:10	02/Sep/2003	05 50
Typhoon	DUJUAN	9	20:10	02/Sep/2003	22:10	02/Sep/2003	02 00
Typhoon	DUJUAN	8SW	22:10	02/Sep/2003	01:30	03/Sep/2003	03 20
Typhoon	DUJUAN	3	01:30	03/Sep/2003	03:20	03/Sep/2003	01 50

Table 3 Summary of the typhoon key parameters during typhoon Dujuan and Imbudo

Name	Date	Time	Lat. (deg)	Long. (deg)	β (deg)	c (m/s)	P_c (hPa)	Δp (hPa)	r_m (km)
Dujuan	03.9.1	0	20.7	125.3	278	7.78	950	60	136.1
		6	20.8	123.7	277	8.53	945	65	107.5
		12	21.1	122.0	283	9.21	940	70	81.8
		18	21.6	120.2	282	10.48	940	70	62.8
	03.9.2	0	21.9	118.0	280	9.61	940	70	40.8
		06	22.2	116.5	282	8.40	950	60	20.4
		12	22.6	114.8	274	9.63	955	55	10.0
		18	22.4	112.8	271	10.33	975	35	77.4
	03.9.3	0	22.7	110.8	279	10.37	996	14	117.5
Imbudo	03.7.23	0	18.4	116.9	290	7.62	945	65	193.5
		6	18.9	115.6	289	7.30	945	65	193.5
		12	19.3	114.2	292	6.94	945	65	193.5
		18	19.9	113.1	306	7.38	940	70	181.9
	03.7.24	0	21.0	111.9	311	9.45	940	70	186.8
		6	22.3	110.3	302	8.95	970	40	156.9
		12	22.9	109.0	293	7.81	980	30	236.9
		18	23.5	107.5	291	6.90	990	20	370.5
	03.7.25	0	23.9	106.5	291	5.53	995	15	265.7

*Note: Lat. and Long. are the position of typhoon center; β is the approach angle indicating the typhoon moving direction; c is the translation velocity of typhoon; P_c is the central pressure of typhoon; Δp is the central pressure difference of typhoon between the central pressure and the ambient pressure; r_m is the radius to maximum winds describing the range of most intensive typhoon wind speed.

Then, all the typhoon key parameters during typhoon Dujuan and Imbudo listed in Table 3 are put into the typhoon wind field model, and the hourly mean wind speed and direction at the east side span of the Stonecutters Bridge can be calculated and compared with the wind field measurement data collected by FGS in Hong Kong at the Stonecutters Bridge site from FMS-WTP.

4.2 Measured wind speed source

The wind field measurement data collected by FGS at the Stonecutters Bridge site from FMS-WTP. The FMS-WTP consists of a 50 m high mast structure with a sensory system being installed on the mast as shown in Fig. 13. The mast was erected at the position close to the east side span of the bridge. The sensory system includes two tri-axial ultrasonic-type anemometers, two bi-axial propeller-type anemometers, two bi-axial accelerometers, three thermometers, one barometer, and one hygrometer. One tri-axial ultrasonic-type anemometer and one bi-axial propeller-type anemometer were installed in parallel at the 50m level, and the rest were at the 30 m level.

The field measurement data provided by Highways Department include the wind speed and wind direction measured by the two propeller anemometers and the three orthogonal wind speed components measured by the two ultrasonic anemometers. The sampling frequency used in the wind field measurements is 4 Hz for the ultrasonic anemometers and 5 Hz for the propeller anemometers. The wind data are recorded and saved into a batch of files of one-hour duration according to the type of anemometer. The wind data provided covered the period from 13 October 2002 until 26 July 2003 together with the wind data recorded during Typhoon Dujuan and Imbudo. Therefore, typhoon wind field during Typhoon Dujuan and Imbudo will be simulated in this part for the comparison convenient.

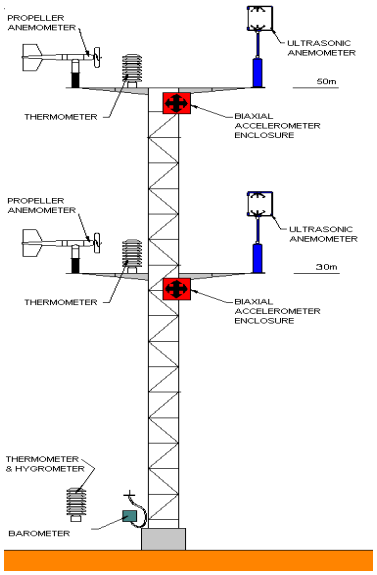

Fig. 13 Sensory system and 50m high mast structure

4.3 Numerical simulation

First, the hourly mean wind speed and direction for typhoon Dujuan and Imbudo are simulated by using the typhoon wind field model.

Then, the hourly mean wind speed and direction for typhoon Dujuan and Imbudo are simulated by using the hybrid simulation method described in the section 2.

4.4 Results and comparison

4.4.1 Comparison of hourly mean wind speed and direction among observed and numerical simulation data during typhoon Dujuan

Fig. 14 shows the comparison of hourly mean wind speed and direction for typhoon Dujuan between the field measurement data and numerical simulation data from 00:00, 1 September to 00:00, 3 September 2003 at the 30 m and 50 m level, respectively. Table 4 shows the error statistics of hourly mean wind speed and direction for typhoon Dujuan between the field measurement data and numerical simulation data at 30 m and 50 m level, respectively.

It can be seen from Fig. 14 that the hybrid numerical simulation method can gives a better prediction to the hourly mean wind speed compared with that simulated by typhoon wind field model within the entire duration of 49 hours except in the 44 hour point at 30 m and 50 level, respectively. The hourly mean wind direction predicted by the hybrid numerical simulation method also gives a good results compared with that gives by the typhoon wind field model except in the 12, 47, 48 hour points. In addition, it can be seen that there exists jumps in the hourly mean wind direction for using typhoon wind field model, which also can be seen in typhoon Imbudo. This is because that only the surface roughness length in conjunction with the typhoon key parameters is used during the simulation of using typhoon wind field model. But by further taking the topography influence into account during the hybrid numerical simulation, the topography has a great influence to the wind direction and this gives a different result with that only using typhoon wind field model. On the other hand, this also demonstrates the necessity of using the hybrid model instead of only using the typhoon wind field model in typhoon wind field simulation. In summary, from Table 4, it can be seen that the hybrid numerical simulation method can gives a better prediction to the hourly mean wind speed and direction compared with the results gives by the typhoon wind field model during typhoon Dujuan at 30 m and 50 m levels, because the effect of topography is taken into account in the hybrid numerical simulation method. In addition, the error between the hybrid numerical simulation method and the field measurement data come from the estimating error of the surface roughness length and the observation error of typhoon key parameters, and all these error sources cause the typhoon wind field simulation error during the simulation process. This also can be found during typhoon Imbudo.

4.4.2 Comparison of hourly mean wind speed and direction among observed and numerical simulation data during typhoon Imbudo

Fig. 15 shows the comparison of hourly mean wind speed and direction for typhoon Imbudo between the observed and numerical simulation data from 00:00, 23 July 2003 to 23:00, 24 July 2003 at the 30 m and 50 m level, respectively. Table 5 shows the error statistics of hourly mean wind speed and direction for typhoon Imbudo between the observed data and numerical simulation data at 30 m and 50 m level, respectively.

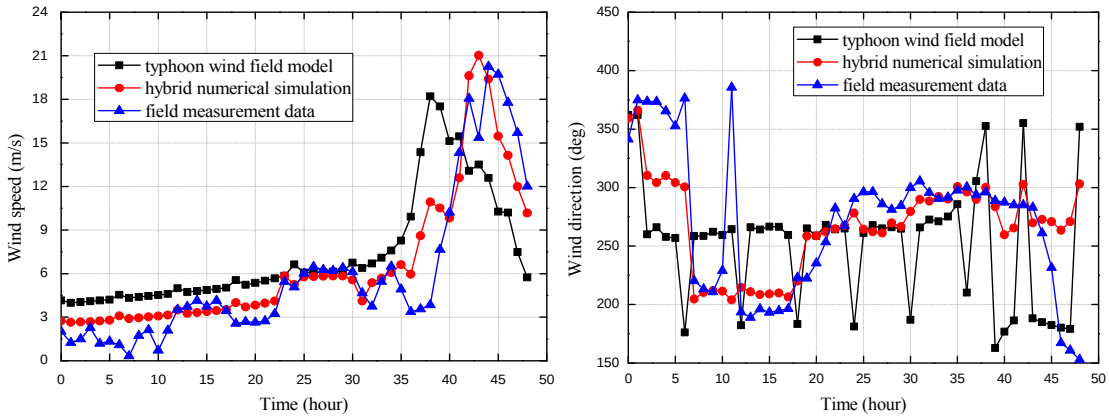

(a) wind speed at the 30 m level (b) wind direction at the 30 m level

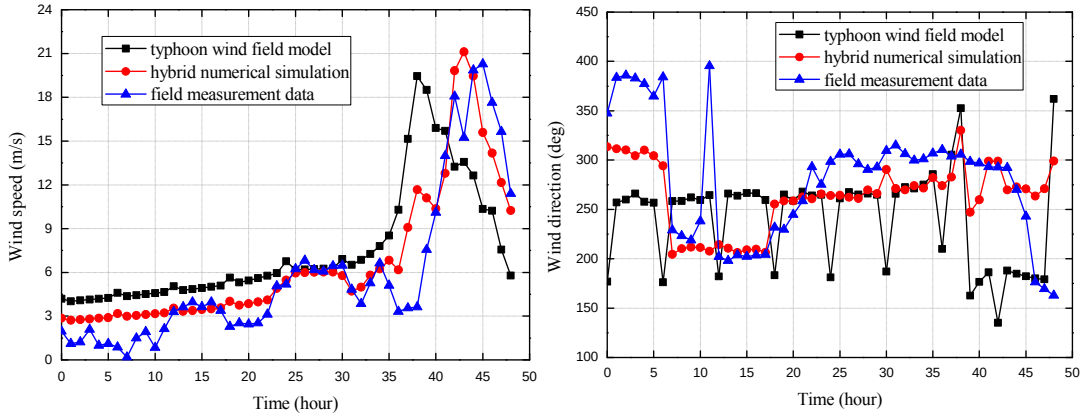

(c) wind speed at the 50 m level (d) wind direction at the 50 m level

Fig. 14 Time series of numerical simulated and observed hourly mean wind speed and direction during typhoon Dujuan

Table 4 Error statistics of hourly mean wind speed and direction for typhoon Dujuan

level	type	Mean wind speed (m/s)			Mean wind speed direction (deg)		
		Max.	Mean	Std.	Max.	Mean	Std.
30m	typhoon model	14.4	3.30	3.12	200	59.6	47.0
	hybrid method	7.08	1.51	1.51	182	29.1	37.6
50m	typhoon model	15.8	3.50	3.29	208	69.6	53.2
	hybrid method	8.04	1.58	1.67	188	37.4	36.2

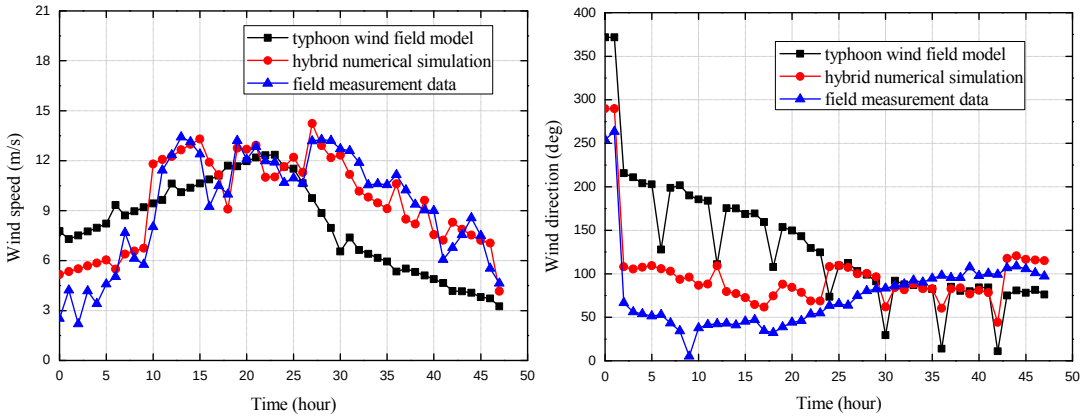

(a) wind speed at the 30 m level (b) wind direction at the 30 m level

(c) wind speed at the 50 m level (d) wind direction at the 50 m level

Fig. 15 Time series of numerical simulated and observed hourly mean wind speed and direction during typhoon Imbudo

Table 5 Error statistics of hourly mean wind speed and direction for typhoon Imbudo

level	type	Mean wind speed (m/s)			Mean wind speed direction (deg)		
		Max.	Mean	Std.	Max.	Mean	Std.
30 m	typhoon model	6.18	2.97	1.74	185	74.4	56.4
	hybrid method	3.78	1.11	0.79	138	43.0	43.2
50 m	typhoon model	6.11	3.04	1.68	156	67.9	48.5
	hybrid method	4.30	1.20	0.95	163	39.7	45.2

It can be seen from Fig. 15 that the hybrid numerical simulation method can gives a better prediction to the hourly mean wind speed compared with that simulated by typhoon wind field model within the entire duration of 49 hours except in the 11 and 17 hour point at 30m and 50 level, respectively. The hourly mean wind direction predicted by the hybrid numerical simulation method also gives a good results compared with that gives by the typhoon wind field model except in the some points gives a little overestimation. In summary, from Table 5, it can be seen that the hybrid numerical simulation method can also give a better prediction to the hourly mean wind speed and direction compared with that gives by the typhoon wind field model during typhoon Imbudo at 30 m and 50 m levels. This also because the effect of topography is taken into account in the hybrid numerical simulation method.

5. Conclusions

A hybrid numerical simulation method for predicting typhoon wind field over complex terrain has been developed in this study. The hybrid numerical simulation method is then applied to the complex terrain around the Stonecutters Bridge in Hong Kong, which is located in a typhoon prone region, as a case study to examine its feasibility and accuracy. In the case study, the average and directional surface roughness lengths for the bridge site were determined based on the DEM information and land use information, and upstream typhoon wind fields for the bridge site were generated based on the typhoon wind field model and typhoon key parameters obtained from HKO. The topographic model for the bridge site within the complex terrain was then established, and the typhoon wind fields at the bridge site were obtained through a series of CFD simulations by taking upstream wind fields as inlets. Typhoon wind fields during typhoon Dujuan and Imbudo are simulated using the hybrid numerical simulation method and typhoon wind field model, and compared with the field measurement data collected by FGS at the bridge site from the FMS-WTP. Case studies demonstrated that the hybrid numerical simulation method can gives a better prediction to the hourly mean wind speed and direction compared with that gives by the typhoon wind field model during typhoon Dujuan and Imbudo at 30 m and 50 m level, because the effect of topography is taken into account in the hybrid numerical simulation method.

Acknowledgements

The work described in this paper was financially funded by China Postdoctoral Science Foundation (2013M540511) and the Fundamental Research Funds for the Central Universities (Hefei University of Technology). The support from the Hong Kong Polytechnic University during the author's PhD study to the author is also appreciated.

References

Batts, M.E., Simiu, E. and Russell, L.R (1980), "Hurricane wind speeds in the United States", *J. Struct. Div.*, **106**(10), 2001-2016.

Bitsuamlak, G.T., Stathopoulos T. and Bedard, C. (2004), "Numerical simulation of wind flow over complex terrain: review", *J. Aerospace Eng.*, **17**(4), 135-145.

Cheng, Y., Lien, F.S., Yee, E. and Sinclair, R. (2003), "A comparison of large eddy simulations with a standard k-ε Reynolds-averaged Navier-Stokes model for the prediction of a fully developed turbulent flow over a matrix of cubes", *J. Wind Eng. Ind. Aerod.*, **91**, 1301-1328.

Chock, G.Y.K. and Cochran, L. (2005), "Modeling of topographic wind speed effects in Hawaii", *J. Wind Eng. Ind. Aerod.*, **93**(8), 623-638.

Georgiou, P.N. (1985), *Design wind speeds in tropical cyclone-prone regions*, PhD Thesis, University of Western Ontario, London, Ontario, Canada.

Hong Kong Observatory (2004),*Tropical cyclone in 2003*, Hong Kong.

Lee, M., Lee, S.H., Hur, M. and Choi, C.K. (2010), "A numerical simulation of flow field in a wind farm on complex terrain", *Wind Struct.*, **13**(4), 375-388.

Maurizi, A., Palma, J.M.L.M. and Castro, F.A. (1998), "Numerical simulation of the atmospheric flow in a mountainous region of the North of Portugal", *J. Wind Eng. Ind. Aerod.*, **74-76**, 219-228.

Meng, Y., Matsui, M. and Hibi, K. (1995), "An analytical model for simulation of the wind field in a typhoon boundary layer", *J. Wind Eng. Ind. Aerod.*, **56**(2-3), 291-310.

Russell, L.R. (1971), "Probability distributions for hurricane effects", *J. Waterw. Harbors Coast. Eng.*, **97**(1), 139-154.

Shen, W.Z., Michelsen, J.A., Sorensen, N.N. and Sorensen, J.N. (2003), "An improved SIMPLEC method on collocated grids for steady and unsteady flow computations", *Numer. Heat Tr. Part B-Fund.*, **43**(3), 221-239.

Tamura, T., Okuno A. and Sugio, Y. (2007), "LES analysis of turbulent boundary layer over 3D steep hill covered with vegetation", *J. Wind Eng. Ind. Aerod.*, **95**(9-11), 1463-1475.

Tryggvason, B.V., Surry, D. and Davenport, A.G. (1976), "Predicting wind-induced response in hurricane zones", *J. Struct. Div.*, **102**(12), 2333-2350.

Vickery, P.J. and Twisdale, L.A. (1995), "Wind field and filling models for hurricane wind speed predictions", *J. Struct. Eng. - ASCE*, **121**(11), 1700-1709.

Vickery, P.J. (2009), "U.S. hurricane wind speed risk and uncertainty", *J. Struct. Eng. - ASCE*, **135**(3), 301-320.

Wakes, S.J., Maegli, T., Dickinson, K.J. and Hilton, M.J. (2010), "Numerical simulation of wind flow over complex terrain", *Environ. Modell. Softw.*, **25**, 237-247.

CC